26 February 2002

Chemical Physics Letters 353 (2002) 325–334

CHEMICAL PHYSICS LETTERS

www.elsevier.com/locate/cplett

Ultrafast electron diffraction of transient cyclopentadienyl radical: A dynamic pseudorotary structure

Hyotcherl Ihee, Jonathan S. Feenstra, Jianming Cao [1], Ahmed H. Zewail *

Laboratory for Molecular Sciences, Arthur Amos Noyes Laboratory of Chemical Physics, California Institute of Technology, Pasadena, CA 91125, USA

Received 12 November 2001

Abstract

Ultrafast electron diffraction (UED) is applied here in the study of the reaction of cylcopentadienyl cobalt dicarbonyl ($CpCo(CO)_2$) which proceeds to give product structures. These structures were probed by picosecond electron pulses. The major product of the fragmentation was found to be the cyclopentadienyl radical. The dynamic nature of the radical was best represented by a pentagonal molecular structure having D_{5h} symmetry with elevated mean amplitudes of vibration. Comparisons between theory and experiment are presented. The structure is that of the transition state between the compressed (dienylic) and the elongated (allylic) conformations but with longer bond distances, reflecting the dynamics of the pseudorotary surface. © 2002 Published by Elsevier Science B.V.

1. Introduction

The cyclopentadienyl radical (Cp), a classic ligand, has long played an important role in different areas of chemistry, both theoretically [1–4] and experimentally [5–8]. Cp is an orbitally degenerate doublet radical subject to a Jahn–Teller distortion into a pair of C_{2v} symmetric conformers joined by a pseudorotary surface. Quantum chemical theory predicts that the Jahn–Teller distortion from the D_{5h} structure stabilizes Cp by 3.5 kcal/mol [2]. The distorted, lower energy ring assumes either a compressed (dienylic) or an elongated (allylic) conformation, which are nearly energetically degenerate (within 0.05 kcal/mol) [2]. Structural deviation from D_{5h} symmetry is large with some previously equal bond lengths now being different by as much as 0.1 Å. However, due to the near energetic degeneracy of the two isomers, Cp exists in a dynamic state of pseudorotation. These interesting electronic properties as well as its transient nature have made Cp attractive to theoretical and experimental inquiry.

Cp is also of interest synthetically where it is present in many important organometallic catalysts. One such compound is cyclopentadienyl cobalt dicarbonyl ($CpCo(CO)_2$), which consists of a Cp ring and two carbonyl ligands bound to a cobalt metal center. What is known about the

* Corresponding author. Fax: +1-626-792-8456.
E-mail address: zewail@caltech.edu (A.H. Zewail).
[1] Present address: National High Magnetic Field Laboratory, Florida State University, 1800 East Paul Dirac Drive, Tallahassee, FL 32310, USA.

0009-2614/02/$ - see front matter © 2002 Published by Elsevier Science B.V.
PII: S0009-2614(01)01476-2

complex structure of ($CpCo(CO)_2$) has been previously determined through studies including the use of microwave spectroscopy [9], X-ray crystal diffraction [10,11], and conventional gas phase electron diffraction (ED) [12]. The photo-induced elimination of carbonyls [13] has also been the focus of some recent work on $CpCo(CO)_2$.

Cp, and many other radical species, are generally unstable and short lived. This often makes conventional experiments aimed at determining their molecular structure not applicable. With this in mind, here we apply ultrafast electron diffraction (UED) which was developed in this laboratory [14–16] to provide the structural information of transient intermediates [17–23]. These UED studies have focused on the structural change in the elimination of an iodine atom from 1,1,2,2-tetrafluoro 1,2-diiodoethane ($C_2F_4I_2$) which results in the formation of the classical intermediate and not the speculated 'bridged' structure [20]. Similarly, the elimination of carbonyls from $Fe(CO)_5$ with products such as $Fe(CO)_4$, $Fe(CO)_2$, $Fe(CO)$ were observed and found to be dependent on the total energy – the transient $Fe(CO)_4$ molecular structure and spin state were determined [17,21]. UED has also been able to observe transients in non-equilibrium thermal states as in the case of the ring opening of 1,3-cylcohexadiene (CHD) [20,22] and in the case of energy redistribution in cylcoheptatriene (CHT) [20,22]. Most recently, the mysterious channel-three process in pyridine was studied and the structure of the open-ring diradical product was characterized [23].

In this Letter, we present our UED results of the fragmentation of gas-phase $CpCo(CO)_2$, a large and complex molecule of 15 atoms. There are three possible reaction channels as illustrated in Scheme 1. Femtosecond and nanosecond multi-photon excitation of $CpCo(CO)_2$ results in a total detachment of all ligands from the cobalt center thereby leaving a bare Cp ring. A subsequent picosecond pulse of electrons allows us to directly observe the molecular structure of the transient species. We were able to discern the product species and establish that it is Cp in a dynamic pseudorotary state. We compare our results with theory and consider the dynamics of the structural changes.

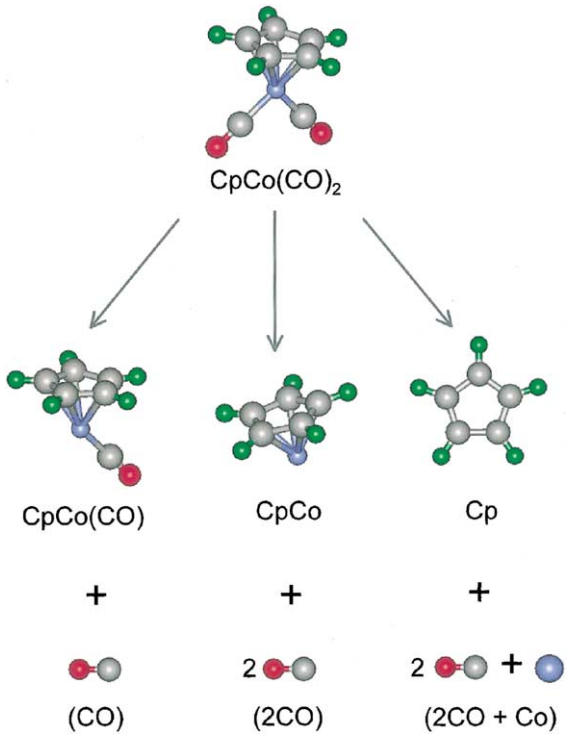

Scheme 1. Three possible fragmentation pathways of $CpCo(CO)_2$.

2. Experimental methods

The second-generation UED apparatus [16] was used for this experiment. It is composed of a femtosecond laser, a picosecond electron gun, a free-jet expansion source, and a two-dimensional single-electron detection system. In a typical UED experiment [16,20], femtosecond laser pulses are used to pump the sample molecules, and similarly we did for this reaction; the reported data, however, were made with nanosecond laser excitation since the product is a long-lived species and we can utilize the much higher energy per pulse; Nd:YAG laser pulses (532 nm, 30 Hz) were directed into a potassium dihydrogen phosphate (KDP) crystal and the resulting frequency-doubled pulses (266 nm, 3 mJ/pulse, 30 Hz) were then directed and focused into the gas sample beneath the needle of the free-jet expansion source in the scattering chamber.

Femtosecond laser pulses from a colliding-pulse mode-locked ring dye laser were amplified in a

four-stage pulsed dye amplifier pumped by the Nd:YAG laser. A part of the amplified pulses (620 nm, 0.5 mJ/pulse, 30 Hz, ~300 fs pulse width) were first frequency-doubled with a KDP crystal, and then focused onto a back-illuminated photocathode in the electron gun to generate ultra-short electron pulses ($\sim 2 \times 10^4$ electrons per pulse with a temporal width of ~15 ps). The ultrashort electron pulses were accelerated to 18.8 keV (de Broglie wavelength is 0.088 Å) and focused into the scattering volume. The two-dimensional diffraction images were recorded with and without the pump laser by a charge-coupled device camera at the end of a phosphor scintillator/fiber optic/image intensifier chain in the detection chamber.

The electron pulse, laser pulse, and molecular beam were arranged in a crossed-beam geometry, and the alignment of the three beams was controlled to within 10 μm. The time-delay between the pumping laser pulses and the probing electron pulses was set at 11 ns. The beam waist of both the electron beam and laser beam was adjusted to be about 300 μm, and the distance between the crossed beams and the detector (camera length) was measured to be 10.24 cm. Data processing was performed with the aid of a computer interface.

$CpCo(CO)_2$ was purchased from Strem Chemical (min. 95% purity) and used without further purification. The sample was transferred into a cell and degassed by three cycles of freeze-pump-thaw. To provide enough molecular gas density in the scattering volume, the sample cell, gas line, and nozzle were heated and the nozzle temperature was maintained at 151 °C. The gas pressure in the scattering chamber during the experiment was about 4×10^{-4} Torr, and the pressure at the scattering volume was estimated to be a few Torr.

3. Computational methods

All calculations were performed using the B3LYP density functional theory (DFT) method in the platform of GAUSSIAN 98 for windows [24]. The 6-311++G** basis set was used to calculate the geometry, vibrational frequencies, and energies of ground state $CpCo(CO)_2$ as well as the isomers of Cp. The 6-31+G* basis set was used to calculate the singlet states of the possible carbonyl eliminated products, CpCoCO and CpCo. The geometry of the triplet state of CpCoCO was taken from a DFT calculation given in the literature [13]. Closed-shell restricted wavefunctions were used for the singlet states and unrestricted wavefunctions were used for calculations involving multiplets.

4. Data analysis

Two-dimensional diffraction images acquired with and without the excitation laser light were radially averaged to generate one-dimensional total intensity curves, I_{tot}, from which experimental modified molecular scattering ($sM(s)$) curves were obtained. Where s is the momentum transfer parameter given by $s = (4\pi/\lambda)\sin(\theta/2)$; λ is the de Broglie wavelength of the incident electrons and θ is the scattering angle.

The diffraction data ($I_{\text{tot}}^{\text{off}}$) recorded without laser light provides a reference signal since it originated from only the ground state parent molecules ($CpCo(CO)_2$). In contrast, the data ($I_{\text{tot}}^{\text{on}}$) obtained with the laser on comprises the contributions from both the remaining parent molecules and newly formed products. Thus, the difference between them selects the reaction change induced by the laser pulse in what we have termed the diffraction–difference method [17]. In the diffraction–difference signal, ($\Delta I_{\text{tot}} = I_{\text{tot}}^{\text{on}} - I_{\text{tot}}^{\text{off}}$), the contributions from unreacted molecules and the background signal, which do not change in the course of the chemical reaction, are eliminated, thus highlighting the signal from structural change.

For data analysis, ΔI_{tot} is converted into the corresponding $\Delta sM(s)$ curve following the conventional definition of $sM(s)$ [25]. The difference radial distribution curve, $\Delta f(r)$, was then obtained by the sine Fourier transformation of the $\Delta sM(s)$ curve. As the difference curves contain equal but opposite contributions from the parent and product structures, it is possible to determine the relative parent and product fractions, whose values reflect the degree of reaction progress [17]. Once this value is obtained from the fitting of the difference curve, the contribution from solely the

product structure can be isolated by adding the appropriately scaled parent diffraction signal to the difference curves. In this product-only curve $(sM(s)_{\mathrm{po}})$, the parent component present in the $\Delta sM(s)$ curve is cancelled out and only the signal from the products remains [18,22].

Before fitting, the raw experimental data (I_{tot}) was divided by the atomic scattering curve obtained by simulating Xenon scattering data to compensate for the s^5 fall-off of the raw data. This modification of the data made it easier to fit a polynomial to the background and therefore obtain a better starting place for structural fitting. The fit was performed in a least-squares manner to minimize the scaled differences (χ^2) between the theoretical $sM(s)$ curve and the experimental one while varying the structural parameters. The structural fitting parameters were in the form of a geometrically consistent z-matrix. This permitted fitting of the whole molecule based on only a few independent variables. The mean amplitudes of vibration (l) of the inter-nuclear distances were approximated using Mastryukov's semi-empirical equations [26,27].

The geometric parameters we present are the result of a partial refinement due to some simplifications intended to eliminate parameter correlation effects in the Cp ring of both the parent and the products. Specifically, the C–H bond distances were not fit and instead taken as given by theory. Also, only one C–C bond and two C–C–C angles in the ring were fit. This allows us to use the one refined bond distance and the two refined angles to derive the rest by geometrical considerations using DFT-determined results for differences between the bond distances and angles. The error bars represent one standard deviation of the least-squares fit. The R values [25] which are often used to represent the goodness of fit for ED data were less than 0.08 for all final refinements reported here; $R < 0.1$ is considered to represent a good fit.

5. Results and discussion

In Fig. 1, we present the modified molecular scattering intensity, $sM(s)_{\mathrm{off}}$, and the radial distribution function, $f(r)_{\mathrm{off}}$, for the parent molecule $\mathrm{CpCo(CO)_2}$ obtained with the pump laser off. The best fit was obtained by floating several parameters of the molecular structure of the parent molecule until reaching the minimum χ^2. The final structural parameters are shown and compared with the results of our density functional calculations. In the analysis of the previous conventional ED experiment [12], it was assumed that the $\mathrm{CpCo(CO)_2}$ had fivefold symmetry for the ring and twofold symmetry as a whole, but our diffraction analysis and electronic structure calculations show that this assumption is an over-simplification.

From our data, the $\mathrm{Co–C_{ring}}$ distances take values of 1.93 and 2.26 Å for the shortest and longest distances, respectively; the average value of all five $\mathrm{Co–C_{ring}}$ distances is 2.09 Å. The DFT values vary from 2.09 to 2.15 Å (average value of 2.13 Å) and a single value (2.12 Å) was reported for all $\mathrm{Co–C_{ring}}$ bonds in the conventional ED [12] analysis. The $\mathrm{Co–C_{ring}}$ distances reported here are more consistent with X-ray crystallographic data; from one report [11], the $\mathrm{Co–C_{ring}}$ bonds are given as 2.01–2.23 Å (average value of 2.09 Å) and from another report [10] the $\mathrm{Co–C_{ring}}$ bonds vary from 2.06 to 2.11 Å (average value of 2.08 Å). The $\mathrm{Co–C_{carbonyl}}$ distance of this work is within one standard deviation of the previous ED data and shorter than the theoretically determined value by 0.067 Å. The C–C bonds within the Cp ligand take values from 1.41 to 1.46 Å and the average value (1.44 Å) is consistent with the only $\mathrm{C_{ring}–C_{ring}}$ bond distance supplied by conventional ED (1.45 Å). Finally, the $\mathrm{C_{carbonyl}–O}$ bond length $(1.211 \pm .015$ Å) is also consistent with the conventional ED data $(1.191 \pm .004$ Å) [12] and longer by 0.064 Å than what is predicted by theory. The main inter-nuclear distances are assigned in the $f(r)_{\mathrm{off}}$ curve in Fig. 1, with excellent agreement between the experimental data and the refined theoretical model.

Next, we consider the diffraction–difference curves in order to establish which reaction channel(s) shown in Scheme 1 is(are) dominant. Fig. 2 shows the comparison between the data and theory for these three possible products. For a starting point, the structural parameters of these different species were obtained from our own DFT calculations and also from the literature [13]. The

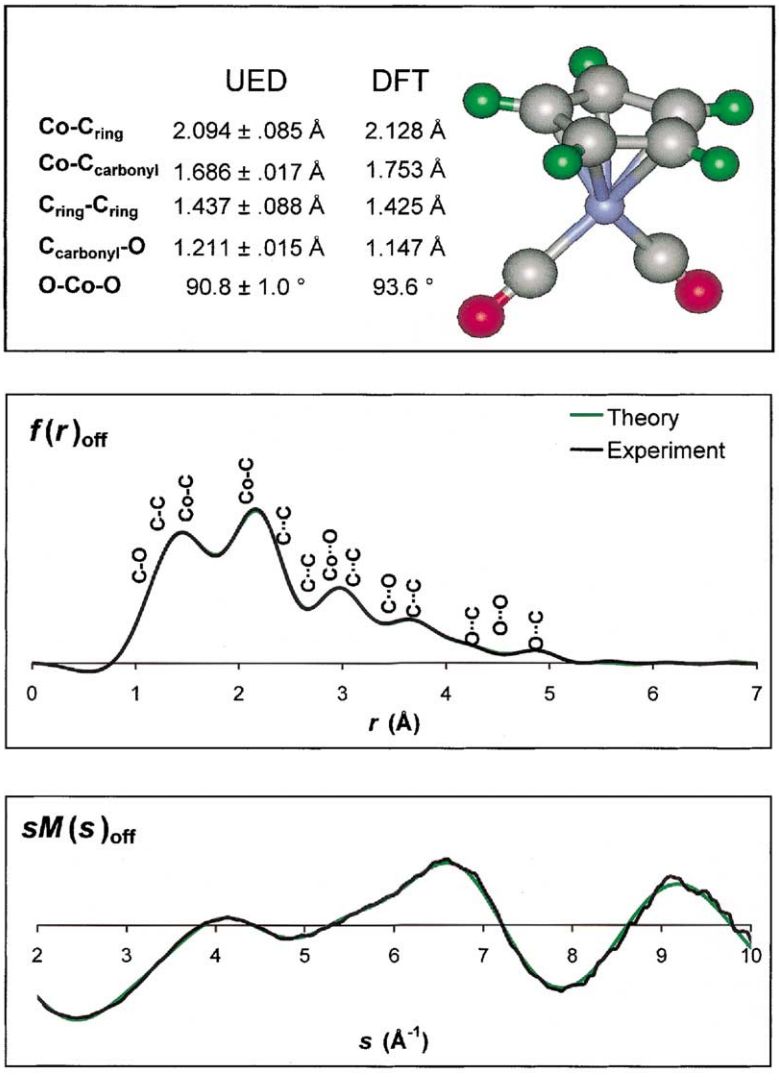

Fig. 1. The refined structure (top) of the parent molecule $CpCo(CO)_2$ along with the modified molecular scattering intensity (bottom) and the radial distribution function (center) obtained with the pump laser off. Black lines are experimental curves and green lines are the least-squares fits. Shown also at the top are our average refined parameters compared with the average parameters from DFT.

contribution from the parent molecule can be cancelled out by adding the appropriate fraction of the parent molecular intensity to these difference curves [18,22]. The resulting product-only curves are shown in Fig. 3. It is clear from both Figs. 2 and 3 that Cp is the main product and that the other reaction product structures are nearly absent. A fit including all three structures was also performed by floating the fraction of each species while keeping their structural parameters fixed at the values obtained from quantum chemical calculations and Cp is overwhelmingly favored.

According to our DFT calculations, the uphill energy for $CpCo(CO)_2$ going to $Cp + Co + 2CO$ is 119 kcal/mol above the ground state of the parent. Our photon energy is 107 kcal/mol and, therefore, with one photon at a wavelength of 266 nm, only carbonyl moieties can be removed. That the Cp

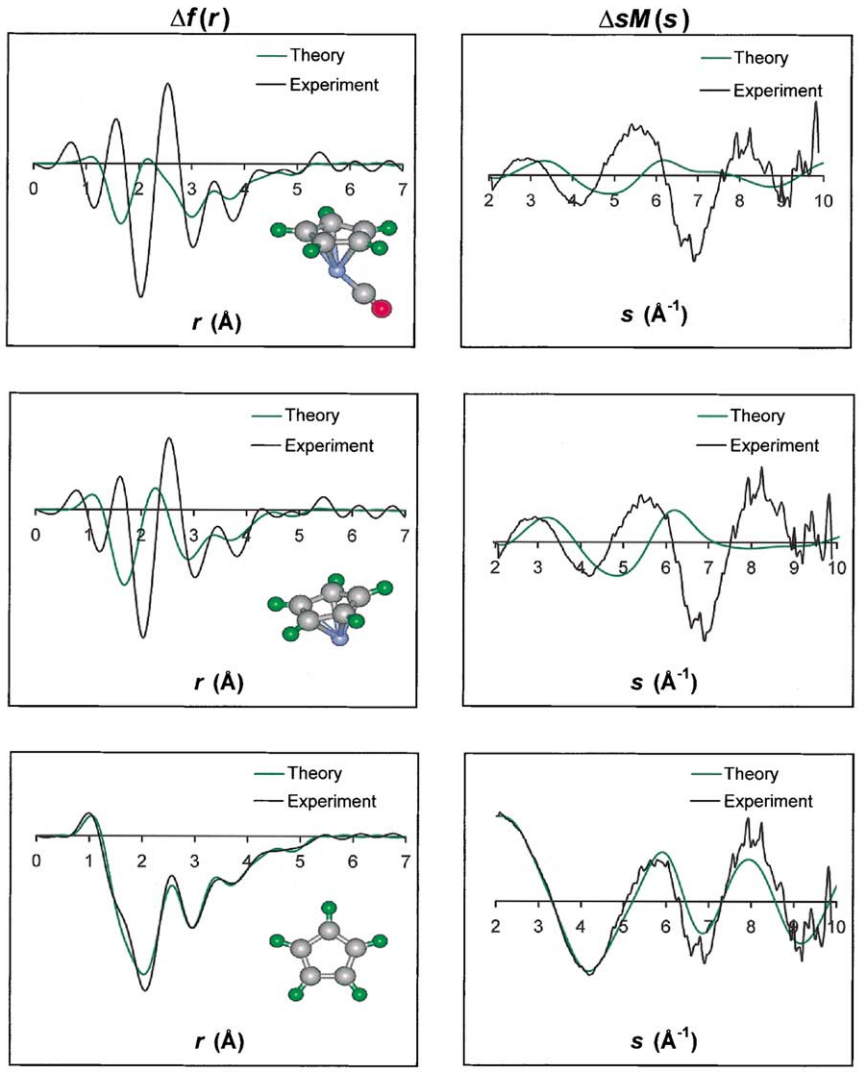

Fig. 2. Comparison between theoretical and experimental fits of the diffraction–difference curve for three possible product channels. Both difference $sM(s)$ curves (right) and $f(r)$ curves (left) are shown. Black lines are experimental curves and green lines are the unrefined theoretical fits. The theoretical curves were obtained from density functional theory calculations. The Cp curve was approximated by a half and half mixture of *elongated* and *compressed* Jahn–Teller isomers, and the fit is not as good as the refined one shown in Fig. 4 (see text).

ring is the main product indicates the reaction is dominated by two-photon processes, consistent with the high pulse energy (3 mJ) used in these experiments. We did not study whether the Cp ring was generated by a simultaneous two-photon absorption or by a successive fragmentation of other intermediates upon further absorption of another photon.

A least-squares fit of the difference curve was performed while varying the structural parameters of the product and the result is shown in Fig. 4. A closer examination of the $\Delta f(r)$ curve reveals the rich details of structural change due to the depletion of $CpCo(CO)_2$ and formation of Cp. The first distinct peak centered at $\sim$2 Å indicates the depletion of Co–$C_{carbonyl}$ and Co–C_{ring} bonds, and the

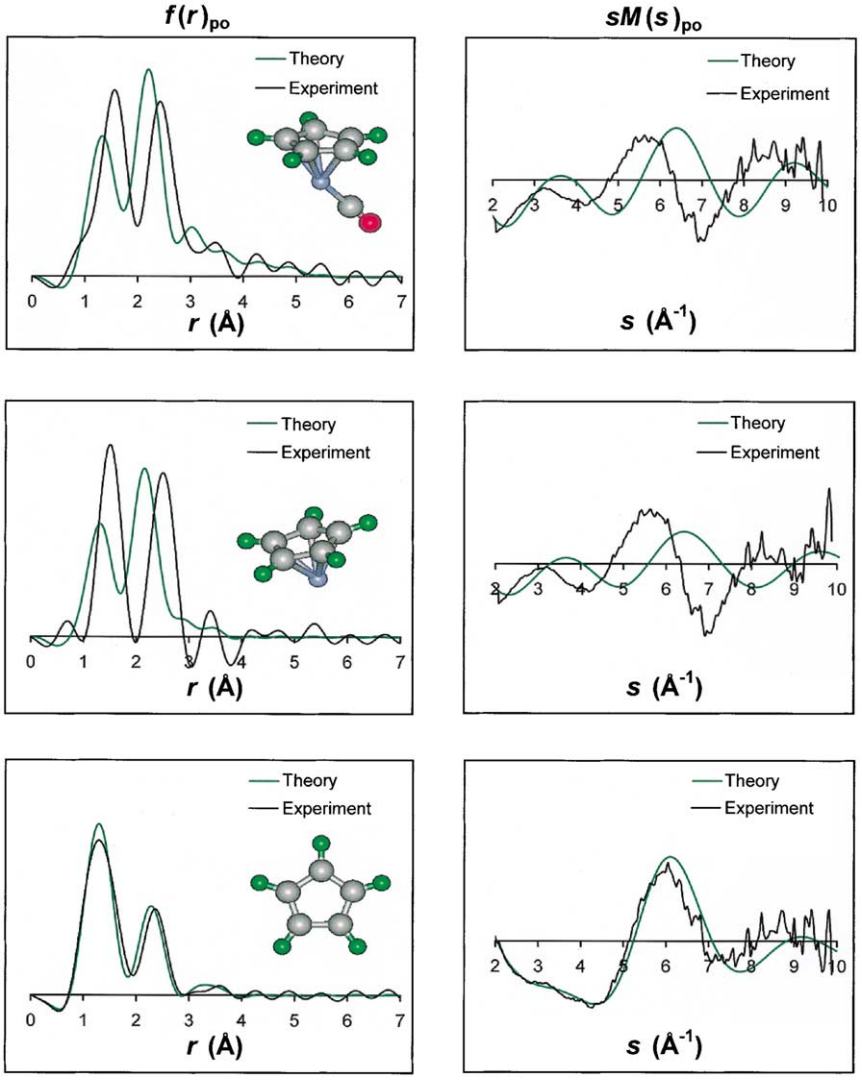

Fig. 3. Comparison between the theoretical and experimental fits of the product-only curve for three possible product channels. Both product-only $sM(s)$ curves (right) and $f(r)$ curves (left) are shown. Black lines are experimental curves and green lines are the unrefined theoretical fits. The theoretical curves were obtained from density functional theory calculations. The Cp curve was approximated by a half and half mixture of *elongated* and *compressed* Jahn–Teller isomers, and the fit is not as good as the refined one shown in Fig. 5 (see text).

second peak centered just below 3 Å indicates the depletion of the $C_{carbonyl} \cdots C_{ring}$ and $Co \cdots O$ distances. The third peak centered at ~3.5 Å indicates the depletion of the $C_{ring} \cdots C_{carbonyl}$ and $C_{ring} \cdots O$ distances, and the last shoulder indicates the depletion of $O \cdots C$ and $O \cdots O$ distances. The first peak corresponding to the $Co–C_{carbonyl}$ and $Co–C_{ring}$ separations clearly shows that the Cp ring and the carbonyls have been separated from the cobalt center.

The product-only structure was refined by a least-squares fit of the product-only curve and the results are shown in Fig. 5. In this curve, the contributions from the parent molecules are completely absent. The product-only $f(r)$ curve, illustrated in Fig. 5, simply shows two peaks: one for

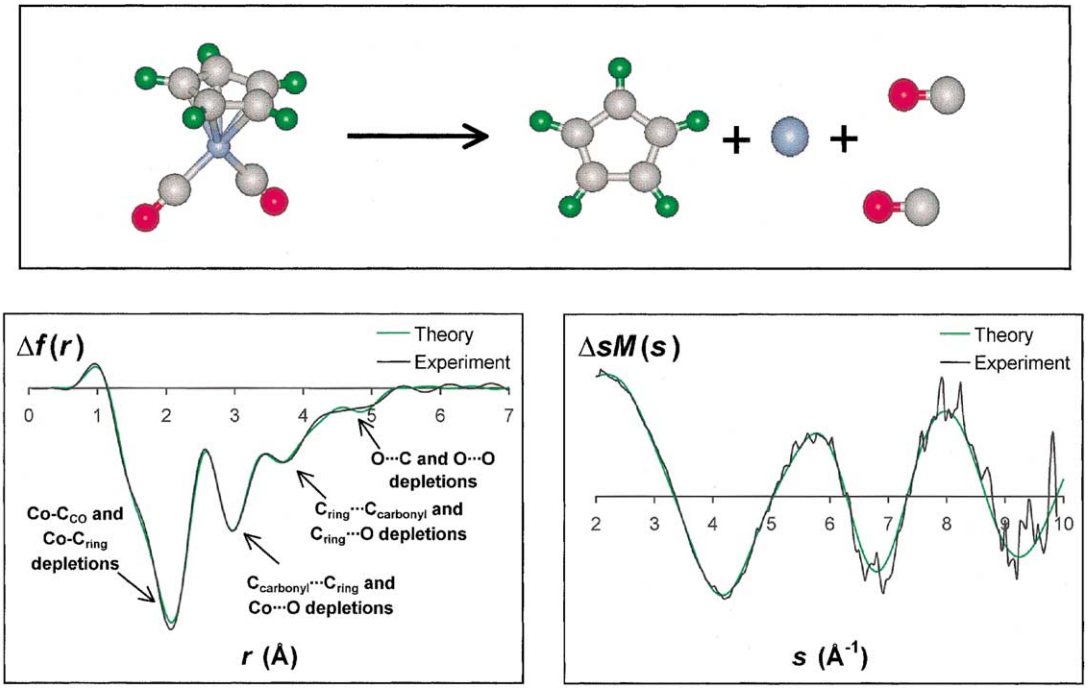

Fig. 4. Refined best fits obtained for the difference curves for the indicated reaction at the top. The bottom-right panel shows the diffraction–difference modified molecular scattering curve and the bottom-left panel shows the diffraction–difference radial distribution curve. Black lines are experimental curves and green lines are the least-squares fits. The top panel shows the molecular structures involved in the reaction.

the C–C bonds at ~1.4 Å and the other for the indirect C···C distances at ~2.3 Å. The final structures obtained from the fit of the diffraction–difference and product-only curve were identical.

In order to examine the nature of dynamic structures, we initially used a 50–50 mixture of the *elongated* and *compressed* Jahn–Teller isomers to fit the difference and product-only diffraction data. However, our final least-squares refinement using the χ^2 criterion yielded results less favorable of a structure composed of two 'static structures', see Figs. 3 and 5. Instead, the fit equilibrium bond lengths (r_e) strayed significantly from the theoretically determined Jahn–Teller structures, indicating the participation of an array of many dynamic structures. This *stretched* ring of D_{5h} symmetry (a regular pentagon) and the large error bars (±0.2 Å for some of the C–C bonds) obtained with a refinement of the 50–50 mixture suggested that another more satisfactory dynamic model was needed to match the data. With this in mind, we used the regular pentagonal structure to represent the dynamics of all conformational change. The DFT electronic structure of D_{5h} Cp was then used as the starting condition for the refinement. The best fit of our data was obtained when the C–C bond of the D_{5h} ring was $r_e = 1.46 \pm 0.003$ Å. DFT gave $r_e = 1.42$ Å, which is consistent with the results from rotationally resolved laser-induced fluorescence spectroscopy [7]. The DFT calculations refer to the bond distance of 1.42 Å of the D_{5h} transition state (see top Fig. 5; center), and we attribute the observed 0.04 Å extension of the equilibrium bond length to the pseudorotary dynamics about the Cp ring.

Cp radical has a degenerate electronic ($^2E_1$) ground state if it is planar, of D_{5h} symmetry; the degeneracy is lifted by Jahn–Teller distortion and the bonds become unequal in length. Due to the near energetic degeneracy of the two Jahn–Teller isomers and the low barrier to pseudorotation on the surface connecting them, the two structures

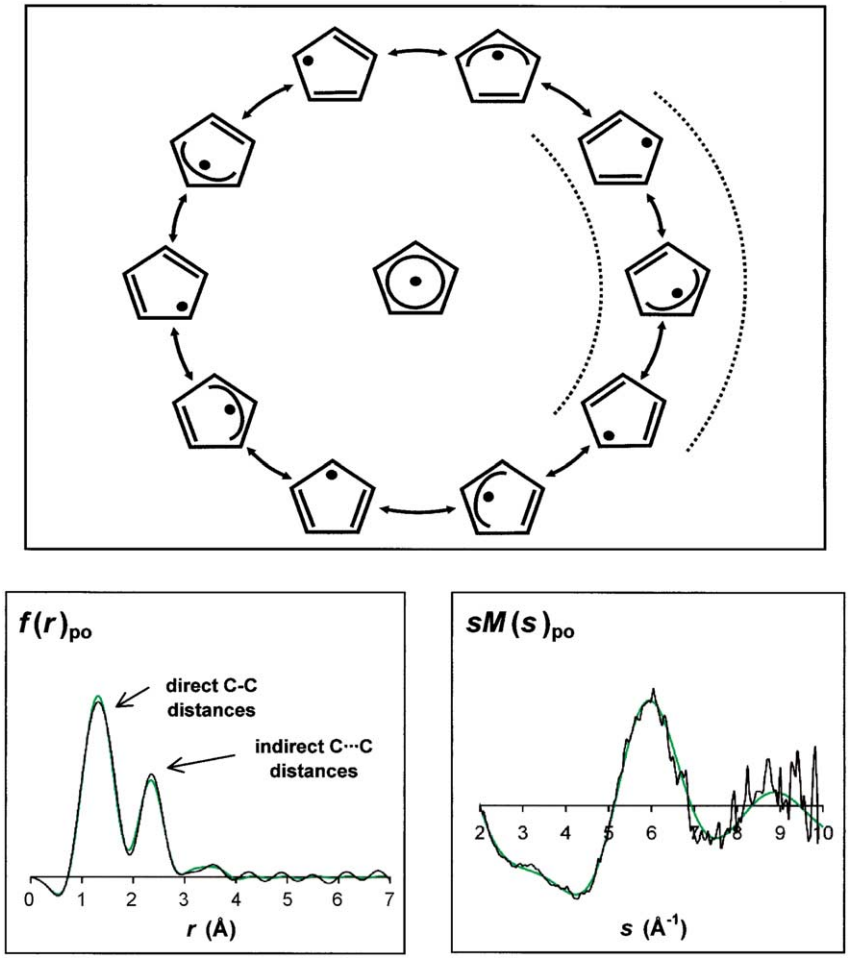

Fig. 5. Top: A representation of pseudorotation in the Cp radical. In the center is the D_{5h} transition state 3.5 kcal/mol [2] above the circular pseudorotary surface connecting the elongated and compressed Jahn–Teller isomers of Cp. The transition states along the circular path are estimated to be elevated by energies ranging from zero to ~2 kcal/mol [6]. The dotted circles indicate two of the many other possible paths. Bottom: The refined best fits obtained for the product-only modified molecular scattering curve ($sM(s)_{po}$) and radial distribution curve ($f(r)_{po}$) of the D_{5h} molecular structure of Cp at 2600 K.The dynamic nature of the radical was best represented by a stretched structure having D_{5h} symmetry with elevated mean amplitudes of vibration.

among the many in Fig. 5 are not static. Estimates of this pseudorotary barrier around the circular landscape (not across the center) in Cp range between zero and ~2 kcal/mol [6]. If no energy is channeled into the translational energies of the fragments, a maximum of ~104 kcal/mol in internal energy for the products is available. If this energy is then completely thermalized between and among all modes of Cp, the vibrational ensemble temperature would be ~2900 K. In reality, however, a significant fraction of the available energy would go into translational kinetic energy of the fragments and the equilibrium temperature of Cp would be lower than this value.

A refinement of the molecular temperature, based on the mean-amplitudes of vibration (l) of the bonds, was also performed and our best-fit temperature of the D_{5h} product was 2600 ± 150 K (see Fig. 5). This apparent high temperature is a consequence of the highly entropic phase space, which results from the many vibrations involved in the transformations of the structures shown (and

not shown) in Fig. 5; note that the arrowed circle represents just one path in the basin of the energy landscape and a few of the many others are represented by dotted circles. The long bonds of the structure and the high vibrational temperature harmonize with the dynamic nature of pseudorotation in this species. An active pseudorotary state involves many bonds changing lengths as the molecule constantly converts between elongated and compressed isomers. The rapid movement of Cp through these pathways at high internal energy is represented by a hot and enlarged D_{5h} structure as obtained by UED, from bond lengths and mean amplitudes of vibration.

Acknowledgements

We wish to thank the National Science Foundation and the United States Air Force Office of Scientific Research for support of this work. We would also like to thank Dr. Boyd Goodson for his helpful discussion.

References

[1] H. Wang, K. Brezinsky, J. Phys. Chem. A 102 (1998) 1530.
[2] K. Pierloot, B.J. Persson, B.O. Roos, J. Phys. Chem. 99 (1995) 3465.
[3] T.-K. Ha, R. Meyer, H.H. Günthard, Chem. Phys. Lett. 69 (1980) 510.
[4] W.T. Borden, E.R. Davidson, J. Am. Chem. Soc. 101 (1979) 3771.
[5] G.R. Liebling, H.M. McConnell, J. Chem. Phys. 42 (1965) 3931.
[6] L. Yu, S.C. Foster, J.M. Williamson, M.C. Heaven, T.A. Miller, J. Phys. Chem. 92 (1988) 4263.
[7] L. Yu, D.W. Cullen, J.M. Williamson, T.A. Miller, J. Chem. Phys. 98 (1993) 2682.
[8] V.A. Korolev, O.M. Nefedov, Russ. Chem. Bull. 42 (1993) 1497.
[9] M.A. Roehrig, Q.-Q. Chen, S.T. Haubrich, S.G. Kukolich, Chem. Phys. Lett. 183 (1991) 84.
[10] M.Y. Antipin, Y.T. Struchkov, A.N. Chernega, M.F. Meidine, J.F. Nixon, J. Organomet. Chem. 436 (1992) 79.
[11] I.W. Nowell, D.R. Russell, J. Chem. Soc., Dalton Trans. (1972) 2393, 2396.
[12] B. Beagley, C.T. Parrott, V. Ulbrecht, G.G. Young, J. Mol. Struct. 52 (1979) 47.
[13] P.T. Snee, C.K. Payne, K.T. Kotz, H. Yang, C.B. Harris, J. Am. Chem. Soc. 123 (2001) 2255.
[14] J.C. Williamson, A.H. Zewail, Proc. Natl. Acad. Sci. 88 (1991) 5021.
[15] M. Dantus, S.B. Kim, J.C. Williamson, A.H. Zewail, J. Phys. Chem. 98 (1994) 2782.
[16] J.C. Williamson, J. Cao, H. Ihee, H. Frey, A.H. Zewail, Nature 386 (1997) 159.
[17] H. Ihee, J. Cao, A.H. Zewail, Chem. Phys. Lett. 281 (1997) 10.
[18] J. Cao, H. Ihee, A.H. Zewail, Chem. Phys. Lett. 290 (1998) 1.
[19] J. Cao, H. Ihee, A.H. Zewail, Proc. Natl. Acad. Sci. USA 96 (1999) 338.
[20] H. Ihee, V.A. Lobastov, U. Gomez, B.M. Goodson, R. Srinivasan, C.-Y. Ruan, A.H. Zewail, Science 291 (2001) 458.
[21] H. Ihee, J. Cao, A.H. Zewail, Angew. Chem. Int. Ed. 40 (2001) 1532.
[22] C.-Y. Ruan, V.A. Lobastov, R. Srinivasan, B.M. Goodson, H. Ihee, A.H. Zewail, Proc. Natl. Acad. Sci. 98 (2001) 7117.
[23] V.A. Lobostov, R. Srinivasan, B.M. Goodson, C. Ruan, J.S. Feenstra, A.H. Zewail, J. Phys. Chem. A 105 (2001) 11159.
[24] M.J. Frisch et al., Gaussian Inc., Pittsburgh, PA, 1998.
[25] I. Hargittai, M. Hargittai, Stereochemical Applications of Gas-Phase Electron Diffraction, VCH, New York, 1988.
[26] V.S. Mastryukov, S.J. Cyvin, J. Mol. Struct. 29 (1975) 15.
[27] V.S. Mastryukov, E.L. Osina, Zhu. Struk. Khim. 17 (1976) 172.